Summary: The synthesis, morphology, and photophysical properties of PF-*b*-PAA with different coil lengths in dilute solutions of dichloromethane/methanol are reported. A tape-like lamellar morphology is observed at a short coil length of PF-*b*-PAA. As the coil length increases, a large compound micelle, sphere, or vesicle is observed with different methanol contents because of the enhancement of the PAA swelling with methanol and the interfacial tension between the PF core and the PAA corona. Upon further increase of the coil length, an inverted morphology of a sphere or rod with a PF corona and PAA core is first observed but the core/corona is then reversed at a high methanol content as a result of the enhanced solubility of PAA. The morphological transformation leads to a significant variation in optical absorption or fluorescence characteristics because of the possible H-aggregate formation.

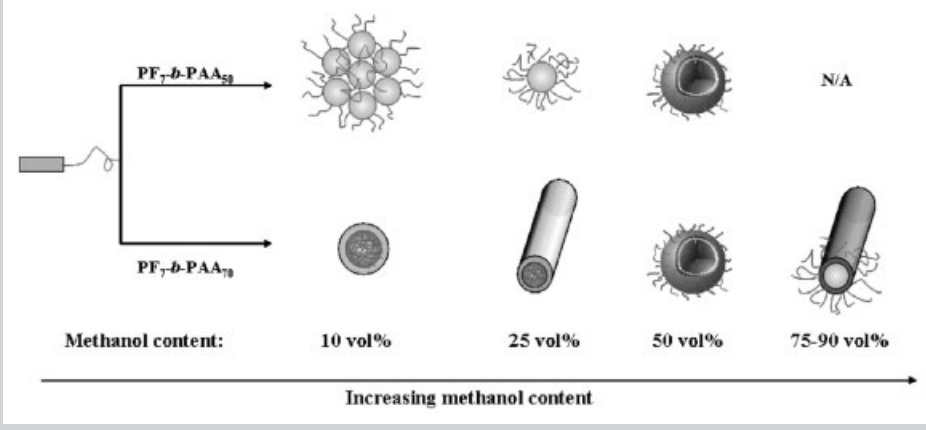

Some of the various morphologies observed upon varying the coil length and the selective solvent content.

Morphological Transformation and Photophysical Properties of Rod-Coil Poly[2,7-(9,9- dihexylfluorene)]-*block*-poly(acrylic acid) in Solution[a]

Yi-Chih Tung,[1] *Wen-Chung Wu,*[1] *Wen-Chang Chen**[1,2]

[1]Department of Chemical Engineering, National Taiwan University, Taipei, Taiwan 106
Fax: +886 2 2362 3040; E-mail: chenwc@ntu.edu.tw
[2]Institute of Polymer Science and Engineering, National Taiwan University, Taipei, Taiwan 106

Received: July 26, 2006; Accepted: August 30, 2006; DOI: 10.1002/marc.200600518

Keywords: diblock copolymers; morphology; photophysics; polyfluorene; rod-coil

Introduction

The self-assembly of rod-coil block copolymers has been demonstrated as a powerful route towards supramolecular objects with novel architectures, functions, and physical

[a] Supporting information for this article is available at the bottom of the article's abstract page, which can be accessed from the journal's homepage at http://www.mrc-journal.de, or from the author.

properties.[1,2] The supramolecular organization of π-conjugated-based rod-coil block copolymers is a topic of great importance because it opens a new way to tune both the molecular organization and electronic and optoelectronic properties of these materials.[3] Aggregation and microphase separation of rod-coil block copolymers have yielded a number of nanoscale morphologies, such as lamellar, spherical, cylindrical, vesicular, and microporous structures.[4] Such morphologies are driven not only by the solvent selectivity but also influenced by the tendency of the rigid segments to aggregate,[4] which differs distinctly from those of conventional coil-coil block copolymers.[5]

Oligo- and polyfluorenes, as well as their derivatives, are excellent candidates for optoelectronic applications because they exhibit high thermal/chemical stability, excellent fluorescence quantum yields, and substantial charge carrier mobility.[6] Several fluorene-based rod-coil and coil-rod-coil block copolymers have been reported.[7] The incorporation of coil segments into the polyfluorene backbones could not only manipulate the electronic and optoelectronic characteristics but also enhance water solubility and generate self-assembly nanostructures, such as sphere, nanoribbon, honeycomb, or wormlike morphologies.[7] However, the above morphologies are observed in the solid state and are mostly characterized by atomic force microscopy. Potential morphological transformations of polyfluorene rod-coil block copolymers induced by coil length and solvent quality have not yet been fully explored.

In this communication, the synthesis, morphology, and photophysical properties of amphiphilic diblock copolymers of poly[2,7-(9,9-dihexylfluorene)]-*block*-poly(-acrylic acid) (PF-*b*-PAA) with three different coil lengths are reported. The chemical structures of the studied PF-*b*-PAA, i.e., PAA_7-*b*-PAA_{26}, PF_7-*b*-PAA_{50}, and PF_7-*b*-PAA_{70}, are shown in Figure 1.

The morphology of PF-*b*-PAA is investigated in dilute solutions of dichloromethane (DCM) and methanol, where DCM is a common solvent for both blocks and methanol is selective for the PAA block. The aggregated morphologies are correlated with the coil length and the selective solvent content. To the best of our knowledge, this is the first time that fluorene-based rod-coil block copolymers with various morphologies of lamellar, sphere, large compound micelle, cylinder, and vesicle, etc, are observed in dilute solutions.

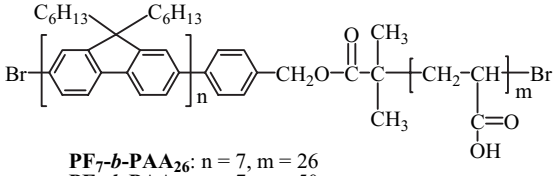

PF_7-*b*-PAA_{26}: n = 7, m = 26
PF_7-*b*-PAA_{50}: n = 7, m = 50
PF_7-*b*-PAA_{70}: n = 7, m = 70

Figure 1. Chemical structures of the synthesized PF-*b*-PAA rod-coil diblock copolymers.

Moreover, the optical absorption and photoluminescence properties of the PF-*b*-PAA are used to understand the aggregation-induced π-π stacking in dilute solution.

Experimental Part

Materials

All of the reagents were purchased from Aldrich or Acros and used as received except for *tert*-butyl acrylate (*t*BA, Aldrich, 98%), which was distilled under vacuum prior to polymerization.

Polymer Synthesis

The polyfluorene macroinitiator, α-{4-[2-(2-bromo-2-methylpropoyloxy)methyl]phenyl}-ω-bromo-poly[2,7-(9,9-dihexylfluorene)] (PF-Br), was synthesized as follows: First, α-(4-hydroxymethylphenyl)-ω-bromo-poly[2,7-(9,9-dihexylfluorene)] was synthesized according to the literature.[7a] It was then reacted with 2-bromoisobutyryl bromide to obtain PF-Br. Poly[2,7-(9,9-dihexylfluorene)]-*block*-poly(*tert*-butyl acrylate) (PF-*b*-PtBA) was synthesized from PF-Br by atom transfer radical polymerization. Taking PF_7-*b*-PAA_{70} as an example, 336 mg (0.06 mmol) of PF-Br, 17.28 mg of CuBr (0.12 mmol), and 3.75 mL of *t*BA (9.6 mmol) were added to a dry round-bottom flask and the system was maintained under vacuum for 10 min. A solution of pentamethyldiethylenetriamine (PMDETA, 25 μL, 0.12 mmol) in 5 mL of anisole was added into the round-bottom flask under nitrogen atmosphere. The mixture was degassed three times, filled with nitrogen, stirred at ambient temperature for 30 min, and immersed into an oil bath at 110 °C for 24 h. After cooling to room temperature, the mixture was passed through an Al_2O_3 column to remove the copper catalyst, precipitated into an excess amount of methanol, filtered off, and the product dried under vacuum at 30 °C to obtain 250 mg of PF-*b*-P*t*BA as a yellow solid. The PF-*b*-P*t*BA was hydrolyzed into PF-*b*-PAA using excess trifluoroacetic acid (TFA). The detailed synthesis procedures, and polymer characterization of PF-Br and three different PF-*b*-PAA copolymers are shown in Supporting Information.

Preparation of PF-b-PAA Aggregates in Solution

PF-*b*-PAA aggregates in solution were prepared by first dissolving the polymer in DCM and then adding methanol with the volume ratios of 10, 25, 50, 75, and 90%, in which the polymer concentration was maintained at 0.1 wt.-% in solution.

Morphology Characterization of Polymer Aggregates in Solution

The PF-*b*-PAA aggregate morphologies were characterized by transmission electron microscopy (TEM) using a JEOL 1210 operating at an acceleration voltage of 100 kV. A drop of the aggregate dispersion was cast onto a 200-mesh copper TEM

grid deposited with carbon and dried under vacuum before imaging.

Results and Discussion

Self-Assembly of PF-b-PAA

Figure 2a–c show representative TEM images of the micellar structures derived from PF_7-*b*-PAA_{26} in a DCM/methanol mixed solvent with methanol contents of 10, 25, and 50 vol.-%, respectively. Because of the low contrast between PAA and the supporting carbon film, the objects in the TEM image represent only the PF domains. All three TEM images exhibit a long strip tape-like structure as the methanol content reaches 50 vol.-%, which is similar to that observed for coil-crystalline polyisoprene-*block*-polyferrocenysilane in solution.[8] Note that PF_7-*b*-PAA_{26} became insoluble if the methanol content was higher than 50 vol.-%. Since the methanol is a poor solvent for PF, the rod PF chains pack as long strips to minimize the interfacial energy between the rod block and methanol. Such structures could result from the PF lamellar domains between solvated PAA chains. While the PF aggregated domains favor ordered packing with their long axes aligned, the corona PAA chains are too short to change the chain conformations by varying methanol contents. Thus, no significant changes in the morphologies of PF_7-*b*-PAA_{26} are observed with increasing methanol contents.

Figure 2d–f show the TEM images of PF_7-*b*-PAA_{50} in a DCM/methanol mixed solvent with methanol volume contents of 10, 25, and 50%, respectively. They exhibit coexisting structures of spherical and large compound micelles (LCMs) with diameters that range from 150 to 400 nm (Figure 2d), spherical micelles with diameters around 150 nm (Figure 2e), and vesicles with 200 nm diameter and a wall thickness of about 25 nm (Figure 2f), respectively. In comparison with the lamella structures of PF_7-*b*-PAA_{26}, these spherical aggregates are favored in the micellization of PF_7-*b*-PAA_{50}. It suggests the significance of the hydrophilic coil length on the morphology of the rod–coil diblock copolymer since the latter has a PAA block length twice that of the former. The entropy loss as a result of the stretching of PAA increases with the chain length, and thus it prefers the spherical aggregate for reducing the PAA stretching. The LCMs shown in Figure 2d probably result from the flocculation or interpenetration of PAA corona at a low methanol content.[9] As the methanol content increases to 25 vol.-%, it enhances the degree of swelling between methanol and PAA and thus reduces the interpenetration of PAA in the corona. Hence, only a simple sphere is formed in Figure 2e. As the solvent becomes more selective for PAA, the interfacial tension between the PF core and PAA corona is increased, which leads to reduced interfacial curvature. Thus, the micelle shape changes from spheres to vesicles in Figure 2f, which is similar to the packing factor mechanism proposed in the literature.[10]

As the PAA coil length increases further, an interesting phase inverse morphology occurs, even at a low methanol content. Figure 3a and 3b show spherical and cylindrical structures of PF_7-*b*-PAA_{70} in DCM/methanol solution with a methanol content of 10 and 25 vol.-%, respectively, in which a bright core of a PAA block is surrounded by a dark corona of PF block. The diameters of the inverted spherical micelles in Figure 3a are about 150–200 nm and the inverted cylinders in Figure 3b have contour lengths ranging from 200 to 500 nm, an average wall thickness of 10 nm, and a core width of 60 nm. The above inverted core/corona morphologies are opposite to those of PF_7-*b*-PAA_{50} shown in Figure 2d and 2e, in which the dark core of PF (electron rich) and the bright corona of PAA (electron poor) are observed. A pure DCM solution of PF_7-*b*-PAA_{70} gradually becomes turbid after stirring because of the limited solubility of the long PAA block in DCM. It suggests that DCM is a good solvent for PF blocks but a slightly poorer solvent for the PAA block in the case of PF_7-*b*-PAA_{70}. Thus, the inverted micelles with a PF corona and PAA core are observed with a methanol content below 25 vol.-%. The morphology transition from spherical (Figure 3a) to cylinder (Figure 3b) is probably because the swelling of the inner PAA core is enhanced with increasing methanol content and leads to an increased interfacial area for cylinder formation.

As the methanol content is further increased to more than 25 vol.-% (Figure 3c to 3e), the solubility of the PAA chains is enhanced and results in aggregates with a PAA corona and a PF inner core. In addition, a significant morphology transformation from inverted cylinder to spherical vesicles and eventually nanorods with increasing methanol content is observed in Figure 3c to 3e, respectively. In Figure 3c, the spherical vesicles appear to be relatively monodisperse in size with a wall thickness similar to those in Figure 2f. Nanorods with contour lengths ranging from 100 to 400 nm and a core diameter of 80 nm are observed at high methanol contents (Figure 3d and 3e). The nanorods with a dark core and bright corona are contrary to the inverted cylinder shown in Figure 3b. The cylindrical structure of these micelles in Figure 3d and 3e might be partly explained by the more cone-shaped conformation of the long chain-based rod-coil molecules[11] and a second driving force might be strong π-π interactions among aromatic segments down the long axis of the rods.[1c]

Photophysical Properties

Figure 4 shows the optical absorption spectra and photoluminescence (PL) spectra of PF_7-*b*-PAA_{70} in a dilute solution of DCM and methanol with methanol contents

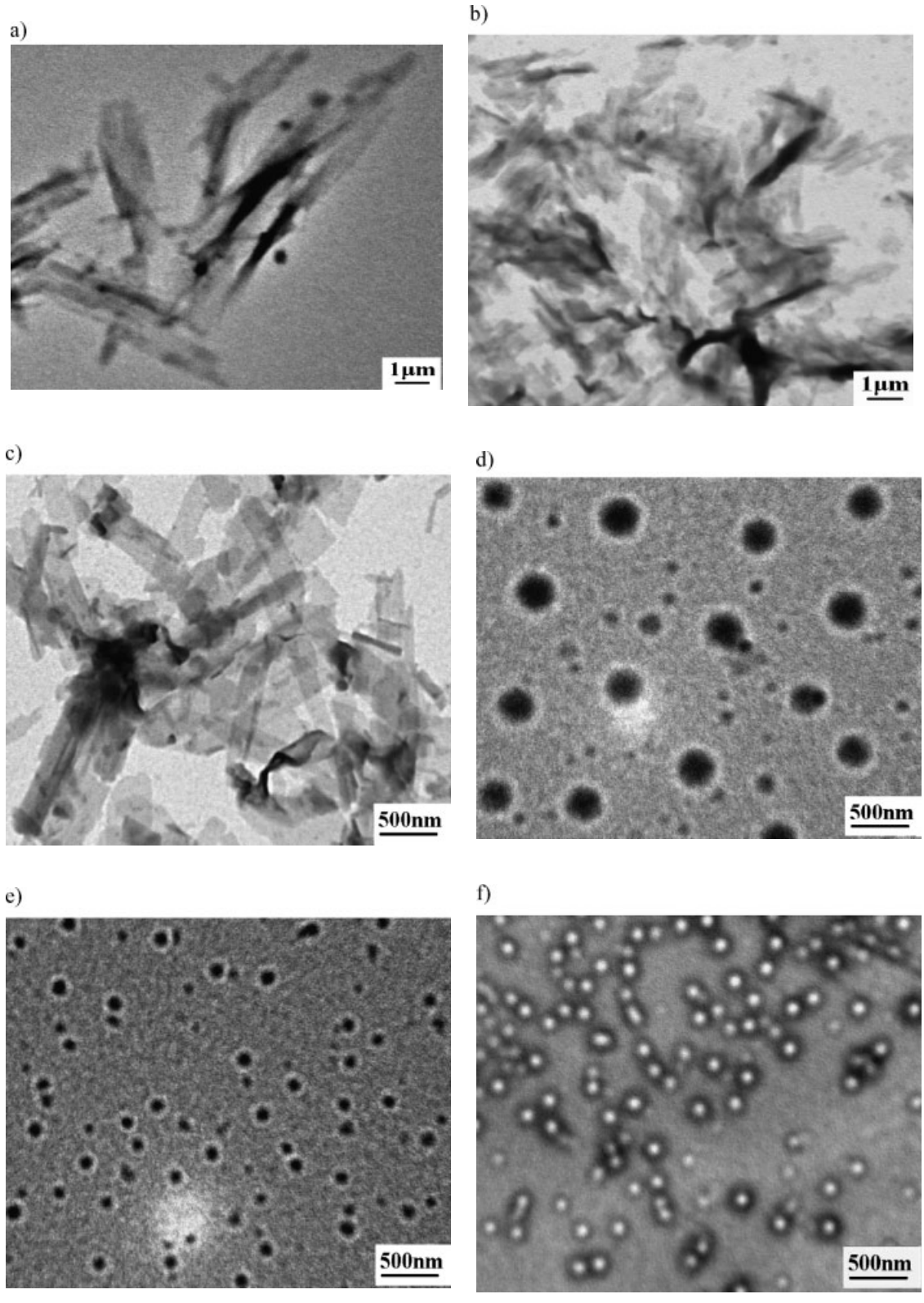

Figure 2. TEM images of PF_7-*b*-PAA_{26} (a–c) and PF_7-*b*-PAA_{50} (d–f) aggregates in dilute solution of DCM and methanol with methanol contents of a,d) 10, b,e) 25, and c,f) 50 vol.-%, respectively.

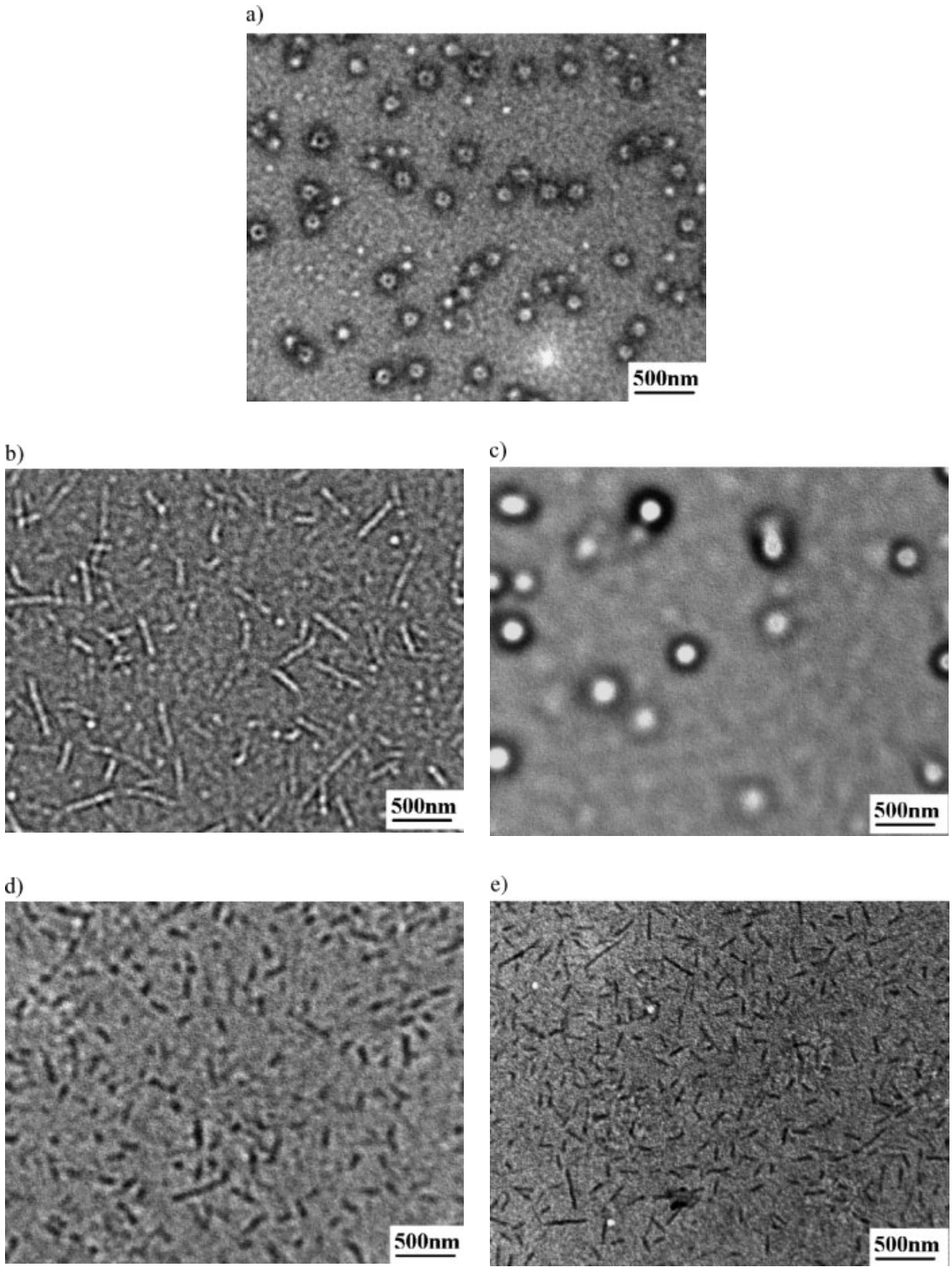

Figure 3. TEM images of PF_7-*b*-PAA_{70} aggregates in dilute solution of DCM and methanol with methanol contents of a) 10, b) 25, c) 50, d) 75, and e) 90 vol.-%, respectively.

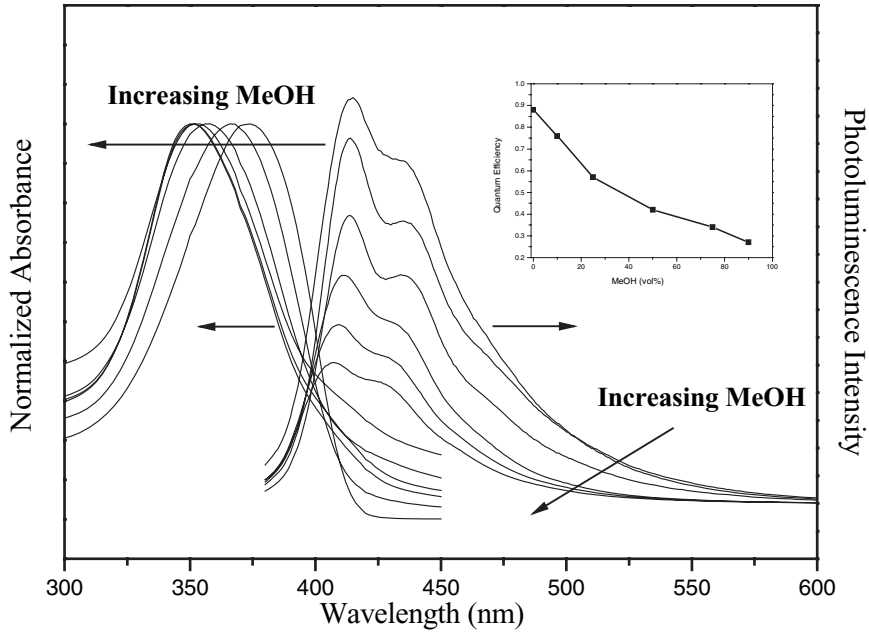

Figure 4. Optical absorption and photoluminescence spectra of PF_7-*b*-PAA_{70} in dilute solution of DCM and methanol with methanol contents ranging from 0 to 90 vol.-%. The inset shows the variation of PL quantum efficiency with methanol content.

ranging from 0 to 90 vol.-%. The inset figure exhibits the variation of PL quantum efficiency with methanol content. As shown in Figure 4, the absorption peak maximum as a result of the π-π^* transition of the PF block shifts from 374 to 350 nm as the methanol content increases from 0 to 90 vol.-%. This blue shift suggests the reduction of the effective conjugated lengths since the PF block becomes less planar on account of the formation of aggregates by its poor solvent of methanol. These phenomena were explained by the molecular exciton model,[12a] assuming H-type aggregation formed by a parallel orientation of PF segments. A similar H-aggregate morphology has also been observed for polyphenyleneethynylene, polythiophene, or oligophenylene vinylene-based rod-coil block copolymers.[12b–d] The intermolecular aggregations of PF-*b*-PAA chains could lead to fluorescence quenching and a hypsochromic (blue) shift in the absorption spectra. The photoluminescence spectra of the aggregates also exhibit dramatic changes, as shown in Figure 4. There are two major emissions at 415 and 435 nm for the PF_7-*b*-PAA_{70} in pure DCM solution. As the methanol content increases to 90 vol.-%, the emission peak at 415 nm is blue-shifted to 407 nm while that at 435 nm is shifted to 426 nm. Such peak shifting is a consequence of interchain π-π interactions between parallel PF blocks, which result from aggregation, and is accompanied by strong fluorescence quenching with a quantum efficiency (ϕ_f) decrease from 0.88 to 0.27 (see insert of Figure 4b). The ϕ_f decreases with further increase of the methanol content and further indicates the H-type aggregation formation of the PF block. In the H-aggregate, the high ordering of the PF block in a parallel orientation is because of the strong π-π interchain interactions. The present study suggests that the aggregate morphologies and photophysical properties of the PF-*b*-PAA rod-coil block copolymers could be tuned through the coil length and the selective solvent content.

Conclusion

Morphologies and photophysical properties of three amphiphilic rod-coil diblock copolymers of PF-*b*-PAA with different coil lengths have been studied. Various morphologies, including lamellar, spheres, large compound micelles, vesicles, cylinders, and inverted spheres and cylinders, are observed by varying the coil length and the selective solvent content. Such morphological transformations could induce the significant variations of optical absorption or fluorescence characteristics because of possible H-aggregation formation. The present study suggests the significance of the rod/coil ratio and selective solvent content on the aggregate morphologies and photophysical properties of the rod-coil block copolymers.

Acknowledgements: We acknowledge the financial support from the *National Science Council of Taiwan*. The helpful discussion with Prof. *H. L. Chen* of the National Tsing-Hua University on the morphology characterization is highly appreciated.

[1] [1a] M. Lee, B. K. Cho, W. C. Zin, *Chem. Rev.* **2001**, *101*, 3869; [1b] P. Leclère, E. Hennebicq, A. Calderone, P. Brocorens, A. C. Grimsdale, K. Müllen, J. L. Brédas, R. Lazzaroni, *Prog. Polym. Sci.* **2003**, *28*, 55; [1c] F. J. M. Hoeben, P. Jonkhijm, E. W. Meijer, A. P. H. J. Schenning, *Chem. Rev.* **2005**, *105*, 1491.

[2] [2a] U. Stalmach, B. de Boer, C. Videlot, P. F. van Hutten, G. Hadziioannou, *J. Am. Chem. Soc.* **2000**, *122*, 5464; [2b] H. Wang, H. H. Wang, V. S. Urban, K. C. Littrel, P. Thiyagarajan, L. Yu, *J. Am. Chem. Soc.* **2000**, *122*, 6855; [2c] J. Liu, E. Sheina, T. Kowalewski, R. D. McCullough, *Angew. Chem. Int. Ed.* **2002**, *41*, 329; [2d] J. F. Hulvat, M. Sofos, K. Tajima, S. I. Stupp, *J. Am. Chem. Soc.* **2005**, *127*, 366.

[3] [3a] M. A. Hempenius, B. M. W. Langeveld-Voss, J. A. E. H. van Haar, R. A. J. Janssen, S. S. Sheiko, J. P. Spatz, M. Möller, E. W. Meijer, *J. Am. Chem. Soc.* **1998**, *120*, 2798; [3b] H. Kukula, U. Ziener, M. Schol, A. Godt, *Macromolecules* **1998**, *31*, 5160; [3c] T. Hayakawa, S. Horiuchi, *Angew. Chem. Int. Ed.* **2003**, *42*, 2285.

[4] [4a] S. A. Jenekhe, X. L. Chen, *Science* **1998**, *279*, 1903; [4b] P. Leclère, A. Calderone, D. Marsitzky, V. Francke, Y. Geerts, K. Müllen, J. L. Brédas, R. Lazzaroni, *Adv. Mater.* **2000**, *12*, 1042.

[5] [5a] P. Alexandridis, B. Lindman, *"Amphiphilic Block Copolymers: Self-Assembly and Applications*", Elsevier, Amsterdam 2000; [5b] N. Hadjichristidis, S. Pispas, G. A. Floudas, *"Block Copolymers: Synthesis Strategies, Physical Properties, and Applications*", Wiley, New Jersey 2003; [5c] D. E. Discher, A. Eisenberg, *Science* **2002**, *297*, 967; [5d] Y. Chen, J. Du, M. Xiong, K. Zhang, H. Zhu, *Macromol. Rapid Commun.* **2006**, *27*, 741; [5e] L. Liu, X. Gao, Y. Cong, B. Li, Y. Han, *Macromol. Rapid Commun.* **2006**, *27*, 260.

[6] [6a] D. Neher, *Macromol. Rapid Commun.* **2001**, *22*, 1365; [6b] U. Schref, E. J. W. List, *Adv. Mater.* **2002**, *14*, 477; [6c] L. L. Chua, J. Zaumseil, J. F. Chang, E. C. Ou, P. K. H. Ho, H. Sirringhaus, R. H. Friend, *Nature* **2005**, *434*, 194.

[7] [7a] D. Marsitzky, M. Klapper, K. Müllen, *Macromolecules* **1999**, *32*, 8685; [7b] S. Lu, Q. L. Fan, S. Y. Liu, S. J. Chua, W. Huang, *Macromolecules* **2002**, *35*, 9875; [7c] P. K. Tsolakis, J. K. Kallitsis, *Chem. Eur. J.* **2003**, *9*, 936; [7d] X. Kong, S. A. Jenekhe, *Macromolecules* **2004**, *37*, 8180; [7e] M. Surin, D. Marsitzky, A. C. Grimsdale, K. Müllen, R. Lazzaroni, P. Leclère, *Adv. Funct. Mater.* **2004**, *14*, 708; [7f] S. Lu, T. Liu, L. Ke, D. G. Ma, S. J. Chua, W. Huang, *Macromolecules* **2005**, *38*, 8494; [7g] C. L. Chochos, J. K. Kallitsis, P. E. Keivanidis, S. Baluschev, V. G. Gregoriou, *J. Phys. Chem. B* **2006**, *110*, 4657; [7h] H. C. Lin, K. W. Lee, C. M. Tsai, K. H. Wei, *Macromolecules* **2006**, *39*, 4298.

[8] L. Cao, M. A. Winnik, I. Manners, *Macromolecules* **2002**, *35*, 8258.

[9] N. S. Cameron, A. Eisenberg, G. R. Brown, *Biomacromolecules* **2002**, *3*, 124.

[10] M. Antonietti, S. Förster, *Adv. Mater.* **2003**, *15*, 1323.

[11] J. N. Israelachvili, "*Intermolecular and Surface Forces*", Academic Press, London 1992.

[12] [12a] M. Kasha, *Radiat. Res.* **1963**, *20*, 55; [12b] K. Li, Q. Wang, *Macromolecules* **2004**, *37*, 1172; [12c] A. de Cuendias, M. Le Hellaye, S. Lecommandoux, E. Cloutei, H. Cramail, *J. Mater. Chem.* **2005**, *15*, 3264; [12d] T. Mori, T. Watanabe, K. Minagawa, M. Tanaka, *J. Polym. Sci., Part A: Polym. Chem.* **2005**, *43*, 1569.

